

## Coordination of Si in Na<sub>2</sub>O-SiO<sub>2</sub>-P<sub>2</sub>O<sub>5</sub> glasses using Si K- and L-edge XANES

DIEN LI,<sup>1,\*</sup> G.M. BANCROFT,<sup>1</sup> AND M.E. FLEET<sup>2</sup>

<sup>1</sup>Department of Chemistry, University of Western Ontario, London, Ontario N6A 5B7, Canada

<sup>2</sup>Department of Earth Sciences, University of Western Ontario, London, Ontario N6A 5B7, Canada

### ABSTRACT

Si K- and L-edge X-ray absorption near-edge structure (XANES) of SiO<sub>2</sub>-P<sub>2</sub>O<sub>5</sub> and Na<sub>2</sub>O-SiO<sub>2</sub>-P<sub>2</sub>O<sub>5</sub> glasses containing P<sub>2</sub>O<sub>5</sub> above 30 mol% were investigated using synchrotron radiation. Both Si K- and L-edge spectra indicate that Si remains fourfold coordinated (<sup>4</sup>Si) with O in these glasses until the content of P<sub>2</sub>O<sub>5</sub> reaches about 32 mol%, at which sixfold coordinated Si (<sup>6</sup>Si) first appears. The proportion of <sup>6</sup>Si increases qualitatively with increase in the content of P<sub>2</sub>O<sub>5</sub>. However, several P<sub>2</sub>O<sub>5</sub>-rich glasses contain <sup>4</sup>Si only, possibly pointing to a dependence of <sup>6</sup>Si content on quench rate. These results are consistent with <sup>29</sup>Si MAS NMR spectra for silicate-phosphate glasses of similar composition. To estimate further the relative proportions of <sup>4</sup>Si and <sup>6</sup>Si in these glasses using Si K-edge spectra, model composite materials of a-SiO<sub>2</sub>, containing <sup>4</sup>Si only, and c-SiP<sub>2</sub>O<sub>7</sub>, containing <sup>6</sup>Si only, were used to establish the correlation of area ratio for <sup>6</sup>Si and <sup>4</sup>Si edge features with bulk composition. The regression equation may be used for semiquantitative estimation of relative proportions of <sup>6</sup>Si and <sup>4</sup>Si in glasses and other materials of unknown structure with compositions similar to those of the present glass systems.

### INTRODUCTION

It is well known that Si is fourfold coordinated (<sup>4</sup>Si) with O in silicates of the Earth's crust but becomes sixfold coordinated (<sup>6</sup>Si) with O at high pressure. For example, silicon dioxide (SiO<sub>2</sub>) has numerous polymorphic modifications with 4:2-coordinated structures (e.g., quartz, cristobalite, and tridymite) and occurs as stishovite with 6:3-coordinated structure at high temperature and pressure beyond about 9 GPa. Materials in the Earth's mantle are believed to be Fe-bearing magnesium silicates, with <sup>4</sup>Si structures dominant in the upper mantle and <sup>6</sup>Si structures dominant in the lower mantle (e.g., Ito and Takahashi 1987; Jeanloz 1990; Finger and Hazen 1991). The phase transformations of Mg<sub>2</sub>SiO<sub>4</sub> and MgSiO<sub>3</sub>, two of the most important silicate components of the mantle, have been established as follows (Liu 1975): with increasing pressure, forsterite (Mg<sub>2</sub>SiO<sub>4</sub>) transforms first to wadsleyite ( $\beta$  spinel), then to ringwoodite ( $\gamma$  spinel), and finally to perovskite plus periclase, whereas enstatite (MgSiO<sub>3</sub>) transforms to  $\beta$  spinel plus stishovite and then to perovskite phases. Crystalline silicon diphosphate (c-SiP<sub>2</sub>O<sub>7</sub>) is one of several compounds in which Si occurs in octahedral coordination with O at atmospheric pressure (e.g., Liebau 1985; Finger and Hazen 1991).

P-bearing silicate glasses and melts have attracted much interest because of their high-technology and geochemical applications. Silica-rich glasses containing P<sub>2</sub>O<sub>5</sub> have been recognized as the most promising fiber material for op-

tical communication systems (Miya et al. 1983). P<sub>2</sub>O<sub>5</sub> also has a profound effect on the evolution of magma systems (Kushiro 1975; Hess 1991; Ryerson and Hess 1978, 1980; London 1987, 1992; London et al. 1990, 1993). For example, the addition of P<sub>2</sub>O<sub>5</sub> to magma leads to liquid immiscibility (Visser and Koster van Groos 1979), significantly depresses the liquidus temperature of magmatic liquids (Wyllie and Tuttle 1964), strongly affects the partitioning of elements between crystals and liquid and between liquid and liquid (Watson 1976), and reduces the viscosity of synthetic granitic liquids (Dingwell et al. 1993).

It has generally been accepted that Si is fourfold coordinated (<sup>4</sup>Si) with O in low-pressure silicate glasses ever since Zachariasen (1932) predicted that the octahedral coordination of Si in glasses would force periodicity and disrupt the vitreous state. Glasses containing P have been studied by IR (Wong and Angell 1976), Raman (Chakraborty and Condrate 1985; Gan and Hess 1992; Gan et al. 1994; Mysen et al. 1981; Nelson and Tallant 1984; Shibata et al. 1981), MAS NMR (Dickinson and De Jong 1988; Dupree et al. 1987, 1989; Gan and Hess 1992; Gan et al. 1994; Sekiya et al. 1988; Weeding et al. 1985), and X-ray absorption near-edge structure (XANES) spectroscopy using synchrotron radiation (Li et al. 1994a, 1995a).

Si appears to remain fourfold coordinated in silicate-phosphate glasses containing <30 mol% P<sub>2</sub>O<sub>5</sub> (Dupree et al. 1989; Okura et al. 1990; Li et al. 1995a). However, the existence of <sup>6</sup>Si in P<sub>2</sub>O<sub>5</sub>-rich glasses is controversial. Chakraborty and Condrate (1985) and Dupree et al. (1987, 1989) reported <sup>6</sup>Si in sodium silicate-phosphate glasses

\* Present address: National Institute of Materials and Chemical Research, Tsukuba, Ibaraki 305, Japan.

**TABLE 1.** Si *K*- and *L*-edge features and compositions of SiO<sub>2</sub>-P<sub>2</sub>O<sub>5</sub> and Na<sub>2</sub>O-SiO<sub>2</sub>-P<sub>2</sub>O<sub>5</sub> glasses

Sample	Composition (mol%)			Si <i>K</i> edge* ( $\pm 0.1$ eV)		Si <i>L</i> edge** ( $\pm 0.1$ eV)			A <sup>[10]</sup> Si**	<sup>[6]</sup> Si
	Na <sub>2</sub> O	SiO <sub>2</sub>	P <sub>2</sub> O <sub>5</sub>	C- <sup>[4]</sup> Si	C- <sup>[6]</sup> Si	A- <sup>[4]</sup> Si	A- <sup>[6]</sup> Si	C- <sup>[4]</sup> Si	A <sup>[6]</sup> Si + A <sup>[4]</sup> Si	<sup>[6]</sup> Si + <sup>[4]</sup> Si
<b>SiO<sub>2</sub>-P<sub>2</sub>O<sub>5</sub> glasses</b>										
52		54.4	45.5	1847.0(3.54)	1848.9(1.29)	105.7	106.6	107.8	0.267	0.139
53		61.7	37.9	1846.9(4.79)	1848.9(0.25)	105.7	106.7	107.8	0.050	0.015
54		50.2	49.6	1847.0(3.59)	1848.9(1.58)	105.7	106.8	107.8	0.306	0.164
5		72.4	27.7	1846.9		105.8		107.9	0	0
<b>Na<sub>2</sub>O-SiO<sub>2</sub>-P<sub>2</sub>O<sub>5</sub> glasses</b>										
40	9.3	31.7	58.9	1846.9(1.81)	1848.9(0.95)	105.6	106.7	107.8	0.344	0.188
43	10.9	31.8	57.2	1846.9(1.68)	1848.9(0.84)	105.6	106.5	107.8	0.333	0.181
45	17.6	49.3	31.7	1846.9		105.6		107.8	0	

\* Edge position (eV) with integrated area (arbitrary units) in parentheses.

\*\* A-<sup>[4]</sup>Si is edge feature; A<sup>[4]</sup>Si represents estimated area of feature.

with P<sub>2</sub>O<sub>5</sub> greater than about 30 mol%, and Sekiya et al. (1988) observed a small amount of <sup>[6]</sup>Si in glass of SiP<sub>2</sub>O<sub>7</sub> composition. However, Chakraborty and Condrate (1985) reported that only <sup>[4]</sup>Si was present in glass of composition SiP<sub>2</sub>O<sub>7</sub>, and similarly Weeding et al. (1985) did not observe <sup>[6]</sup>Si in glasses in the SiO<sub>2</sub>-P<sub>2</sub>O<sub>5</sub> system. Also, Dupree et al. (1989) observed a strong dependence of <sup>[6]</sup>Si on Na<sub>2</sub>O content, with <sup>[6]</sup>Si decreasing to zero at composition 2SiO<sub>2</sub>·3P<sub>2</sub>O<sub>5</sub> and quench conditions.

In a previous paper, we reported Si *K*- and *L*-edge XANES of SiO<sub>2</sub>-P<sub>2</sub>O<sub>5</sub> and Na<sub>2</sub>O-SiO<sub>2</sub>-P<sub>2</sub>O<sub>5</sub> glasses containing <30 mol% P<sub>2</sub>O<sub>5</sub>. The results indicated that Si remains fourfold coordinated in these glasses, but Na<sub>2</sub>O depolymerizes and P<sub>2</sub>O<sub>5</sub> copolymerizes the silicate glasses (Li et al. 1995a). In this paper, we present Si *K*- and *L*-edge XANES spectra of SiO<sub>2</sub>-P<sub>2</sub>O<sub>5</sub> and Na<sub>2</sub>O-SiO<sub>2</sub>-P<sub>2</sub>O<sub>5</sub> glasses containing >30 mol% P<sub>2</sub>O<sub>5</sub>. Using model composite materials prepared from mixtures of amorphous silica (a-SiO<sub>2</sub>) and crystalline silicon diphosphate (c-SiP<sub>2</sub>O<sub>7</sub>), we establish a correlation between the relative intensities of <sup>[4]</sup>Si and <sup>[6]</sup>Si edge peaks and bulk composition and are able to estimate semiquantitatively the relative proportions of <sup>[4]</sup>Si and <sup>[6]</sup>Si in these two glass series.

## EXPERIMENTAL METHODS

Crystalline silicon diphosphate (c-SiP<sub>2</sub>O<sub>7</sub>) was synthesized by reacting high-purity amorphous SiO<sub>2</sub> (a-SiO<sub>2</sub>; commercial vitreous silica) and excess H<sub>3</sub>PO<sub>4</sub> in an open silica-glass tube at initially 230 °C and finally about 950 °C. The product was identified as the monoclinic P2<sub>1</sub>/n phase by powder X-ray diffraction (XRD). Glasses in the system Na<sub>2</sub>O-SiO<sub>2</sub>-P<sub>2</sub>O<sub>5</sub> were prepared from mixtures of Na<sub>2</sub>Si<sub>2</sub>O<sub>5</sub>, c-SiP<sub>2</sub>O<sub>7</sub>, and P<sub>2</sub>O<sub>5</sub> contained in a silica-glass tube. The starting composition was separated from the silica-glass wall by a sleeve of platinum foil. Each sample was maintained vertically in a box furnace, heated at 1200 °C for about 10 min, and quenched in water. Glasses in the system SiO<sub>2</sub>-P<sub>2</sub>O<sub>5</sub> were prepared from mixtures of c-SiP<sub>2</sub>O<sub>7</sub>, a-SiO<sub>2</sub>, and P<sub>2</sub>O<sub>5</sub> contained as above, heated at 1400–1500 °C for 5–7 min, and quenched in water. Glasses were examined by optical microscopy and pow-

der XRD, and glass compositions were determined by electron microprobe analysis (EMPA) (see Table 1). All glasses were optically transparent, isotropic and inclusion free, X-ray amorphous, and compositionally homogeneous. A series of model composite materials containing both <sup>[4]</sup>Si and <sup>[6]</sup>Si was made by mechanically mixing accurately weighed proportions of a-SiO<sub>2</sub> and c-SiP<sub>2</sub>O<sub>7</sub>. The model composite materials and glass samples were ground into very fine powder (about 10 μm) for the Si *K*- and *L*-edge XANES measurements.

Si *K*-edge XANES spectra of the model composite materials and glasses were collected with a double-crystal monochromator (DCM) using InSb(111) monochromator crystals, giving an energy resolution of 0.8 eV at 1840 eV (Yang et al. 1992). Si *L*-edge XANES spectra were recorded using a Grasshopper beamline that employs a grazing incidence system with a grating of 1800 grooves/mm (Bancroft 1992). The resolution of the Grasshopper beamline is about 0.1 eV at 100 eV. For both Si *K*- and *L*-edge measurements, very fine powder samples were spread uniformly on electric carbon tape supported on a stainless steel sample holder. The area covered by the sample was about 10 mm in diameter for Si *K*-edge measurements, and the sample thickness was constant for the measurements of each sample. Both Si *K*- and *L*-edge spectra were recorded by total electron yield (TEY), which measures the sample current of electrons of different energies that escape from the surface because of excitation by synchrotron X-rays. The TEY spectrum is proportional to the absorption coefficient, μ.

All samples were prepared in a similar manner to minimize the effects of sample thickness and particle size on the relative intensity of absorption features. Three measurements were made for each sample. The spectrum for each measurement was normalized by  $I/I_0$ , where  $I$  is the intensity of the TEY signal and  $I_0$  is the intensity of the photon flux. The raw spectrum for each sample investigated was averaged from three normalized measurements and smoothed. A linear preedge background was removed from each spectrum. All Si *K*-edge XANES spectra were calibrated against the Si *K* edge of α-quartz at 1846.8 eV, and all Si *L*-edge spectra were calibrated by

the Si *L* edge (peak a) of  $\alpha$ -quartz at 105.7 eV (Li et al. 1994b). The fitting of the Si *K*-edge spectra into Gaussian components was carried out using the BAN data analysis program (Tyliszczak 1992).

## RESULTS AND DISCUSSION

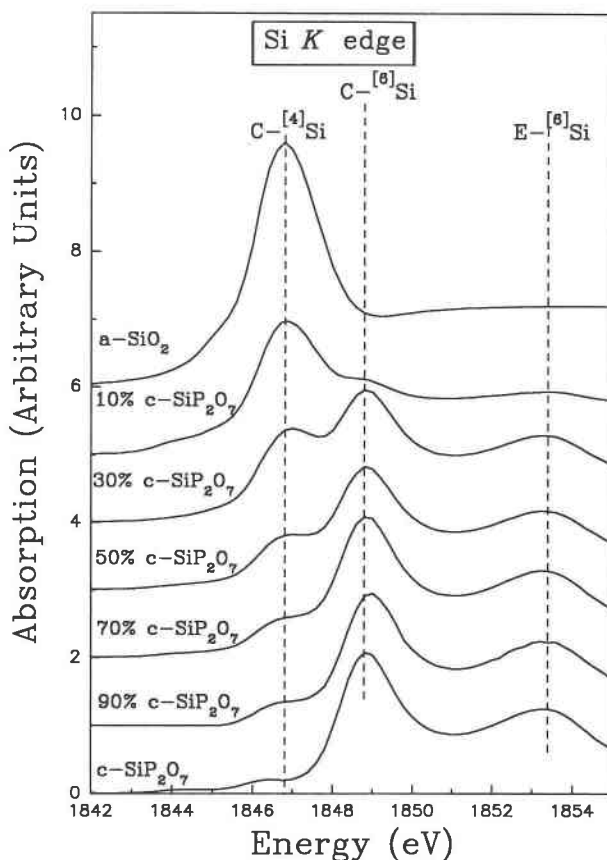
### Si *K*-edge XANES spectra of a-SiO<sub>2</sub>-c-SiP<sub>2</sub>O<sub>7</sub> model composite materials

Figure 1 shows the Si *K*-edge XANES spectra of a-SiO<sub>2</sub>, c-SiP<sub>2</sub>O<sub>7</sub>, and the model composite materials prepared from mixtures of a-SiO<sub>2</sub> and c-SiP<sub>2</sub>O<sub>7</sub>. The spectrum of a-SiO<sub>2</sub>, which contains <sup>28</sup>Si only, is dominated by a major peak at 1846.9 eV, whereas the spectrum of c-SiP<sub>2</sub>O<sub>7</sub>, which contains <sup>30</sup>Si only, is characterized by a major peak at 1848.9 eV. The absorption features are labeled as in our previous work (Li et al. 1994b). It is apparent that, as expected, the relative intensity of peak C-<sup>28</sup>Si increases and the relative intensity of peak C-<sup>30</sup>Si decreases with increasing proportion of a-SiO<sub>2</sub> in the model composite materials.

The major peak in the a-SiO<sub>2</sub> spectrum has been assigned by many researchers to a 1s → 3p transition in the SiO<sub>4</sub> tetrahedra of silicate and aluminosilicate materials (Lagarde et al. 1992; Li et al. 1994b; Fröba et al. 1995a, 1995b). Similarly, peak C-<sup>30</sup>Si in c-SiP<sub>2</sub>O<sub>7</sub> has been assigned to a 1s → 3p transition in SiO<sub>6</sub> octahedra (Li et al. 1994b). These peaks are of the same type as the discrete resonances observed in tetrahedral SiX<sub>4</sub> molecules (1s → 3p-like t<sub>2</sub> states) and in the octahedral SiF<sub>6</sub> molecule (1s → 3p-like t<sub>1g</sub> states; Lagarde et al. 1992; Sutherland et al. 1993). Full multiple-scattering calculations on a SiO<sub>4</sub> cluster can also rationalize these peaks as the result of single-scattering resonances in the SiO<sub>4</sub> tetrahedra (Lagarde et al. 1992). The peaks at higher energy, in the immediate postedge region (e.g., E-<sup>30</sup>Si at ~1853 eV), result from a combination of multiple-scattering and shape resonances (e.g., Lagarde et al. 1992; Li et al. 1994b; Fröba et al. 1995a).

The Si *K*-edge spectra for the model composite materials were interpreted by subtracting the spectrum for a-SiO<sub>2</sub> and then fitting the features of the separate <sup>28</sup>Si and <sup>30</sup>Si spectra into the Gaussian components. In Figure 2a, the dotted line is the experimental spectrum of a model composite sample containing 70 mol% a-SiO<sub>2</sub> and 30 mol% c-SiP<sub>2</sub>O<sub>7</sub>. Peak C-<sup>28</sup>Si in the Si *K*-edge spectrum of a-SiO<sub>2</sub> (solid line) was normalized to the height of peak C-<sup>28</sup>Si in the spectrum of the model sample, so that the difference (dashed line) between the model sample and the a-SiO<sub>2</sub> represents the features for <sup>30</sup>Si. The absorption features for both <sup>28</sup>Si and <sup>30</sup>Si were fitted into the Gaussian components, as shown in Figures 2b and 2c, respectively. The upper dot lines are absorption features for <sup>28</sup>Si and <sup>30</sup>Si, the dashed lines are the fitted Gaussian components, and the solid curves are the envelopes of the fitted components. Backgrounds (lower dot lines) were included in the fitting procedures.

The integrated areas (arbitrary units) for the <sup>28</sup>Si-edge peak (C-<sup>28</sup>Si) and the <sup>30</sup>Si-edge peak (C-<sup>30</sup>Si) in the spectra



**FIGURE 1.** Si *K*-edge XANES spectra of model composite materials prepared from mechanical mixtures of a-SiO<sub>2</sub>, containing <sup>28</sup>Si only, and c-SiP<sub>2</sub>O<sub>7</sub>, containing <sup>30</sup>Si only. The relative intensity of the <sup>28</sup>Si edge peak at 1846.9 eV increases, and that of the <sup>30</sup>Si edge peak at 1848.9 eV decreases proportionally with increasing a-SiO<sub>2</sub>.

of all model composite materials were derived from the fitting procedures. The normalized areas for <sup>28</sup>Si (squares) and <sup>30</sup>Si (dots) edge peaks are plotted against the content (mole percent) of <sup>28</sup>Si and <sup>30</sup>Si, respectively, in Figures 3a and 3b. The error for the quantity <sup>30</sup>Si/(<sup>30</sup>Si + <sup>28</sup>Si) is estimated to be about 5%, and the errors for the areas of <sup>28</sup>Si- and <sup>30</sup>Si-edge peaks are estimated to be about 8%. The correlation between the area for the <sup>30</sup>Si-edge peak and the composition is inferior to that for <sup>28</sup>Si, partly because the absorption features for <sup>30</sup>Si were derived from the difference spectrum between the model composite materials and a-SiO<sub>2</sub>.

It is evident that the correlation of normalized area of the <sup>30</sup>Si-edge peak with proportion of <sup>30</sup>Si in the model composite materials is markedly nonlinear (Fig. 3). This may be attributable simply to a higher absorption cross section for <sup>30</sup>Si than for <sup>28</sup>Si. If this is the case, the calibration curves of Figure 4 could be used to determine <sup>30</sup>Si content in all materials, regardless of their bulk composition. Theoretically, the absorption coefficient,  $\mu$ , is proportional to the number of absorbing Si atoms,  $N_{Si}$ ,

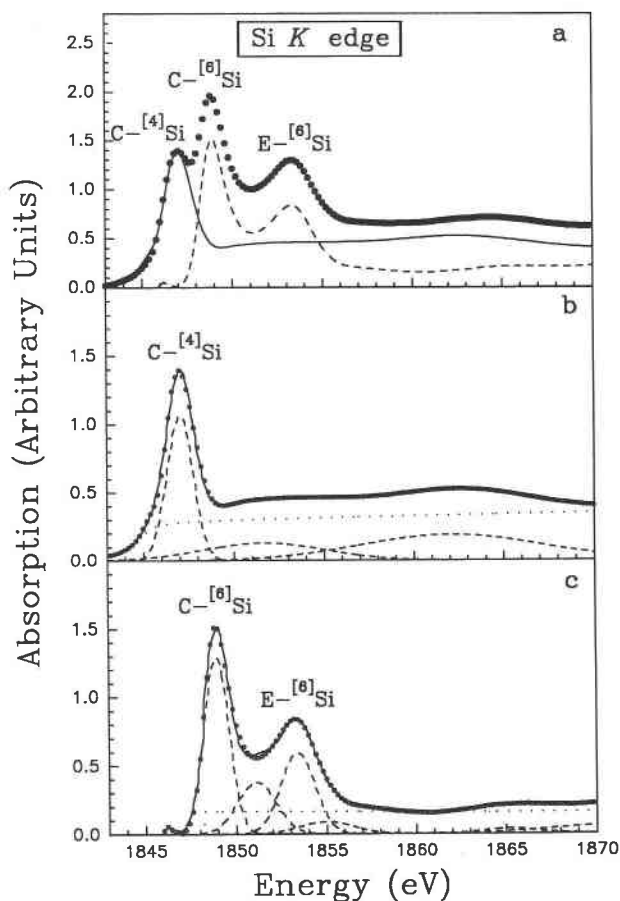


**FIGURE 2.** Data reduction for Si *K*-edge XANES spectrum of a model composite material containing 70 mol% a-SiO<sub>2</sub> and 30 mol% c-SiP<sub>2</sub>O<sub>7</sub>. (a) The dotted line is the experimental Si *K*-edge spectrum. Peak C-<sup>[4]</sup>Si in the Si *K*-edge spectrum (solid line) of a-SiO<sub>2</sub> was normalized to the height of peak C-<sup>[4]</sup>Si in the end-member spectrum, so that the difference spectrum (dashed line) represents the absorption features for <sup>[6]</sup>Si. (b and c) The absorption features for <sup>[4]</sup>Si (a-SiO<sub>2</sub>) and <sup>[6]</sup>Si (c-SiP<sub>2</sub>O<sub>7</sub>), respectively, were fitted into the Gaussian components. Upper dot lines are the absorption features for <sup>[4]</sup>Si and <sup>[6]</sup>Si; dashed lines are the fitted Gaussian components; solid lines are the envelopes of the fitted components; lower dot lines are the fitted backgrounds.

and the absorption cross section,  $\sigma$ .  $N_{\text{Si}}$  is dependent on the concentration of Si in the samples and on experimental conditions. In our technique for the quantification of <sup>[4]</sup>Si and <sup>[6]</sup>Si, the experimental conditions (particle size and thickness of samples, and the spot size of the synchrotron X-ray beam) were reasonably constant for the Si *K*-edge measurements of both model materials and glasses. In this case,  $N_{\text{Si}}$  is related only to the concentration of Si in the samples. On the other hand, the absorption cross section,  $\sigma$ , is different for <sup>[4]</sup>Si and <sup>[6]</sup>Si and is actually unknown theoretically. The Si *K*-edge spectra of the model a-SiO<sub>2</sub> and c-SiP<sub>2</sub>O<sub>7</sub> materials indicated that  $\sigma$  is generally larger for <sup>[6]</sup>Si than for <sup>[4]</sup>Si, even though the exact values of  $\sigma$  for <sup>[4]</sup>Si and <sup>[6]</sup>Si cannot be derived. Thus,

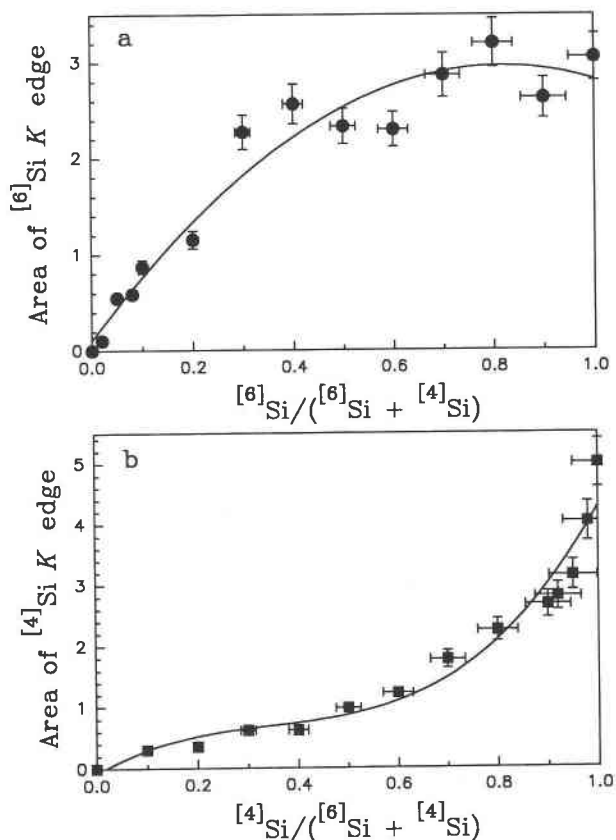


**FIGURE 3.** The integrated areas (or relative intensities) of <sup>[6]</sup>Si (dots) (a) and <sup>[4]</sup>Si (squares) (b) edge peaks correlated with atomic proportion of species in model composite materials. Error in composition was estimated to be about 5%, and the errors for the integrated areas were estimated to be about 8%. The solid lines were fitted by least-squares regression.

the absorption intensity is not expected to be linearly correlated with the concentration of <sup>[4]</sup>Si and <sup>[6]</sup>Si species.

However, our experience suggests that the present calibration may be applied only to materials of bulk composition similar to the SiO<sub>2</sub>-P<sub>2</sub>O<sub>5</sub> system. As one comparison, the Si *K*-edge XANES spectrum of wadeite-structured K<sub>2</sub>Si<sub>4</sub>O<sub>9</sub> (Swanson and Prewitt 1983) gives 22% <sup>[6]</sup>Si from a simple comparison of the areas of the C-<sup>[4]</sup>Si and C-<sup>[6]</sup>Si peaks. Figure 4 has the convex-upward form of a typical relative intensity vs. concentration calibration curve for the quantitative analysis of powder mixtures by XRD (e.g., Klug and Alexander 1974). The densities of a-SiO<sub>2</sub> and c-SiP<sub>2</sub>O<sub>7</sub> are 2.19 and 3.05 g/cm<sup>3</sup>, respectively. However, we do not know whether the non-linearity of the present calibration curve is due to attenuation of either primary synchrotron radiation or the Auger electrons and electron cascade.

The absolute values for absorption intensity measured in the spectra are very dependent on sample preparation (particle size and thickness, etc.) and the spot size of the synchrotron radiation beam. It is difficult to keep these experimental parameters constant for each sample, but

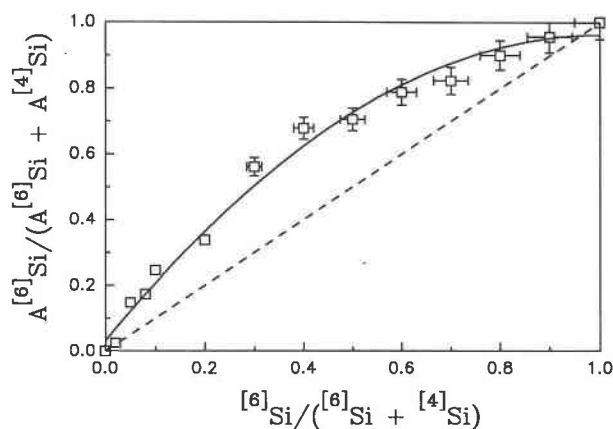


**FIGURE 4.** Correlation of peak area ratio for  $^{60}\text{Si}$  and  $^{44}\text{Si}$  with atomic proportion of species in model composite materials. Error in the area ratio was estimated to be about 5%. The solid line was fitted with experimental data (open squares) by least-squares regression, and the dashed line represents the ideal proportional correlation. An empirical equation was derived for the model materials and may be used for the quantification of  $^{60}\text{Si}$  and  $^{44}\text{Si}$  in glasses and other materials of unknown structure.

their effects are minimized by using the peak-area ratio in Figure 4. The error in the quantities  $A^{[6]}\text{Si}/(A^{[6]}\text{Si} + A^{[4]}\text{Si})$  and  $^{[6]}\text{Si}/(^{[6]}\text{Si} + ^{[4]}\text{Si})$  shown in this figure was estimated to be about 5%. The solid line is the corresponding correlation curve defined by the regression equation  $y = -0.9160x^2 + 1.8476x + 0.0314$ , with a correlation coefficient of 0.9947, where  $y = A^{[6]}\text{Si}/(A^{[6]}\text{Si} + A^{[4]}\text{Si})$ ;  $x = ^{[6]}\text{Si}/(^{[6]}\text{Si} + ^{[4]}\text{Si})$ . This correlation equation may be used to estimate the relative proportions of  $^{44}\text{Si}$  and  $^{60}\text{Si}$  in glasses and other materials of unknown structure that are closely comparable in composition to the  $\text{SiO}_2\text{-P}_2\text{O}_5$  system.

#### Si *K*- and *L*-edge XANES spectra of $\text{SiO}_2\text{-P}_2\text{O}_5$ and $\text{Na}_2\text{O-SiO}_2\text{-P}_2\text{O}_5$ glasses

Figure 5 shows Si *K*-edge XANES spectra of  $\text{SiO}_2\text{-P}_2\text{O}_5$  (Fig. 5a) and  $\text{Na}_2\text{O-SiO}_2\text{-P}_2\text{O}_5$  (Fig. 5b) glasses. For both series of glasses, when the content of  $\text{P}_2\text{O}_5$  is less than about 32 mol%, only peak C- $^{44}\text{Si}$  is observed, indicating that Si remains fourfold coordinated. When the content of  $\text{P}_2\text{O}_5$  is greater than 32 mol%, the other two prominent peaks C- $^{60}\text{Si}$  and E- $^{60}\text{Si}$  are observed, indicating that some Si atoms are in octahedral coordination with O. The assignments of peaks C- $^{44}\text{Si}$ , C- $^{60}\text{Si}$ , and E- $^{60}\text{Si}$  are similar to those described in the last section (Li et al. 1994b). Qualitatively, the relative intensities of both peaks C- $^{60}\text{Si}$  and E- $^{60}\text{Si}$  increase with increase in  $\text{P}_2\text{O}_5$  content, indicating an increase in the relative proportion of  $^{60}\text{Si}$ .

Figure 6 shows the corresponding Si *L*-edge XANES spectra of these  $\text{SiO}_2\text{-P}_2\text{O}_5$  (Fig. 6a) and  $\text{Na}_2\text{O-SiO}_2\text{-P}_2\text{O}_5$  (Fig. 6b) glasses. These are in good agreement with the Si *K*-edge spectra for both series of glasses. When the content of  $\text{P}_2\text{O}_5$  is less than about 32 mol%, only peaks A- $^{44}\text{Si}$  and C- $^{44}\text{Si}$  are evident, indicating that Si is fourfold coordinated (see also Li et al. 1994a). When the content of

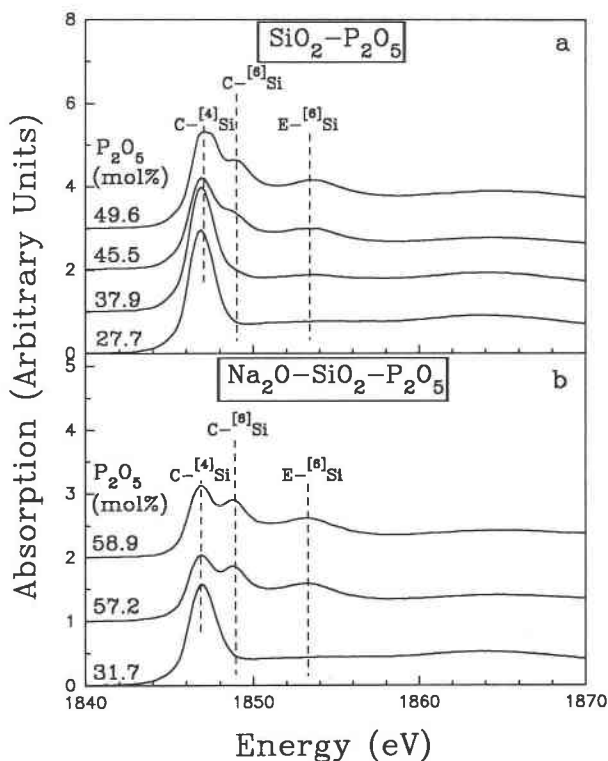


**FIGURE 5.** Si *K*-edge XANES spectra of  $\text{SiO}_2\text{-P}_2\text{O}_5$  (a) and  $\text{Na}_2\text{O-SiO}_2\text{-P}_2\text{O}_5$  (b) glasses. The absorption features are labeled as in our previous paper (Li et al. 1994b).

$\text{P}_2\text{O}_5$  is greater than 32 mol%, another prominent peak A- $^{60}\text{Si}$  is observed, indicating that some Si atoms are in octahedral coordination. As described in our previous paper (Li et al. 1994a), peak A- $^{44}\text{Si}$  is assigned to the transition of  $^{44}\text{Si}$  2p electrons to the unoccupied  $^{44}\text{Si}$  3s-like  $a_1$  states, and peak C- $^{44}\text{Si}$  to the transition of  $^{44}\text{Si}$  2p electrons to the unoccupied  $^{44}\text{Si}$  3p-like  $t_2$  states. Also, peak A- $^{60}\text{Si}$  is assigned to the transition of  $^{60}\text{Si}$  2p electrons to the unoccupied  $^{60}\text{Si}$  3s-like  $a_{1g}$  states (Li et al. 1994b).

Thus, both Si *K*- and *L*-edge XANES spectra indicate a change in coordination of some Si atoms in both  $\text{SiO}_2\text{-P}_2\text{O}_5$  and  $\text{Na}_2\text{O-SiO}_2\text{-P}_2\text{O}_5$  glasses when the content of  $\text{P}_2\text{O}_5$  increases beyond 32 mol%, and the content of  $^{60}\text{Si}$  increases in proportion to the increase in the content of  $\text{P}_2\text{O}_5$ . The Si *K*-edge peak of silicate minerals containing only  $^{44}\text{Si}$  has been shown to shift to higher energy with increase in the polymerization of  $\text{SiO}_4^{4-}$  clusters (Li et al. 1995b). Although the features due to the structural units of different polymerizations are not well resolved, the Si *K*-edge peak of diopside glass shifts to lower energy and becomes much broader, indicating that the diopside glass contains structural units from  $\text{Q}^0$  to  $\text{Q}^4$  (Li et al. unpublished manuscript). However, Si *K*- and *L*-edge peaks for  $^{44}\text{Si}$  in the glasses investigated remain essentially constant in energy positions (see Table 1) and have similar line widths, indicating that the  $\text{SiO}_4^{4-}$  cluster has similar polymerization and distortion, even though the content of

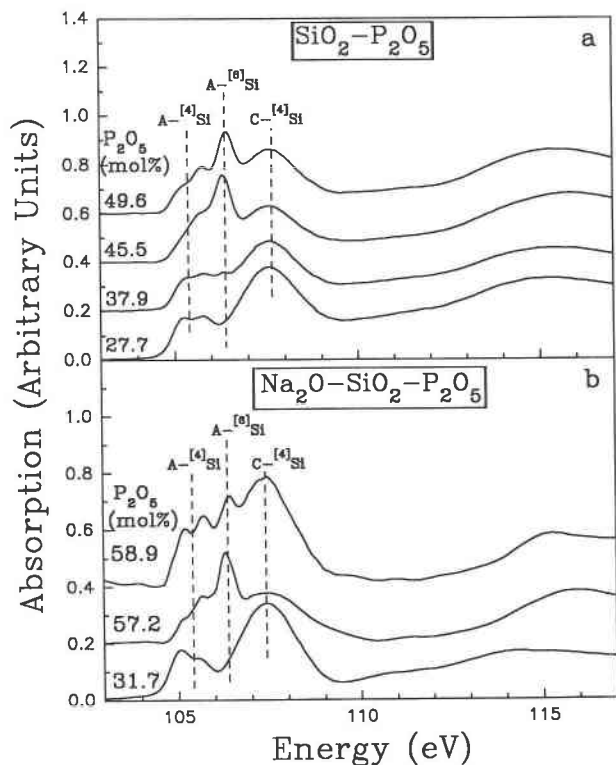


FIGURE 6. Si *L*-edge XANES spectra of  $\text{SiO}_2\text{-P}_2\text{O}_5$  (a) and  $\text{Na}_2\text{O-SiO}_2\text{-P}_2\text{O}_5$  (b) glasses. The absorption features are labeled as in our previous paper (Li et al. 1994b).

$\text{SiO}_2$  ranges between 32 and 72 mol%. All these results are in good agreement with  $^{29}\text{Si}$  MAS NMR spectra of similar silicate-phosphate glass systems (Dupree et al. 1987, 1989; Sekiya et al. 1988).

To estimate more quantitatively the relative proportions of  $^{44}\text{Si}$  and  $^{60}\text{Si}$  in these glasses, the Si *K*-edge XANES spectra were reduced as described in the previous section for the model composite materials. Peak C- $^{44}\text{Si}$  in the spectrum of a- $\text{SiO}_2$  was normalized to the height of peak C- $^{44}\text{Si}$  in the spectrum of each glass, so that the difference spectrum between the glass sample and a- $\text{SiO}_2$  represents the absorption features for  $^{60}\text{Si}$ . The absorption features for both  $^{44}\text{Si}$  and  $^{60}\text{Si}$  were fitted into the corresponding Gaussian components, and the areas (or relative absorption intensities) for both  $^{44}\text{Si}$  and  $^{60}\text{Si}$  edge peaks were derived. Then the empirical equation derived from the model composite materials was used to calculate the relative proportions of both  $^{60}\text{Si}$  and  $^{44}\text{Si}$  (Table 1).

Figure 7 shows the variation of the proportion of  $^{60}\text{Si}$  with the content of  $\text{P}_2\text{O}_5$  in both  $\text{SiO}_2\text{-P}_2\text{O}_5$  and  $\text{Na}_2\text{O-SiO}_2\text{-P}_2\text{O}_5$  glasses, as determined in this study and by Li et al. (1995a). For both series of silicate-phosphate glasses, Si remained fourfold coordinated with O at low  $\text{P}_2\text{O}_5$  content. However, beyond about 32 mol%, a bimodal distribution is evident. About one-half of our  $\text{P}_2\text{O}_5$ -rich glasses yielded spectra with  $^{60}\text{Si}$ , giving a composition-dependent distribution similar to that in Figure 5 of Du-

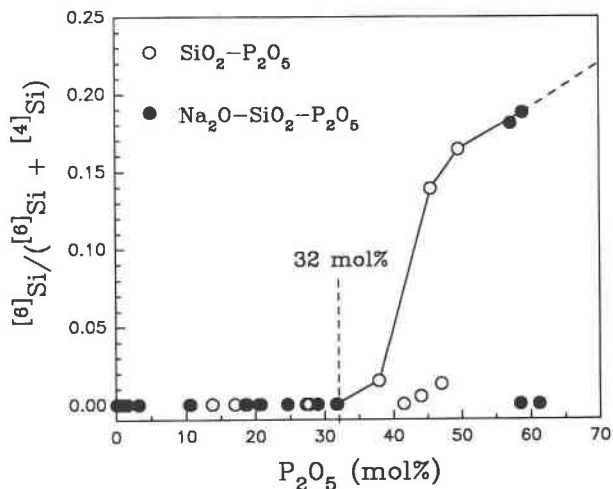


FIGURE 7. Atomic proportion of  $^{60}\text{Si}$  as a function of  $\text{P}_2\text{O}_5$  content in  $\text{SiO}_2\text{-P}_2\text{O}_5$  (open circles) and  $\text{Na}_2\text{O-SiO}_2\text{-P}_2\text{O}_5$  (solid circles) glasses. The threshold value of  $\text{P}_2\text{O}_5$  for stabilizing  $^{60}\text{Si}$  in these glasses appears to be about 32 mol%. Data for  $\text{P}_2\text{O}_5$  contents of less than 30 mol% are from Li et al. (1995a).

pre et al. (1989) for glasses of composition  $\text{Na}_2\text{O}\cdot 2\text{SiO}_2\cdot p\text{P}_2\text{O}_5$  ( $p = 0.26\text{--}4.0$ ). However, other samples in both glass series investigated did not have features of  $^{60}\text{Si}$  in their Si *K*-edge XANES spectra. The XANES spectra for these samples were recollected using new sample aliquots during a subsequent beam time but were unchanged.

There are two possible explanations for this unusual behavior. First, the glass samples in question may have gained moisture, which either degraded the glasses directly or induced surface damage during sample preparation: XANES collected by TEY largely reflect surface and near-surface structure. Second, the glass samples in question may not have contained  $^{60}\text{Si}$  because either the content of  $^{60}\text{Si}$  in these glass compositions is sensitive to quenching conditions or the starting materials were incompletely reacted. We experienced great difficulty making small amounts of the  $\text{P}_2\text{O}_5$ -rich glasses and resorted to the sealed silica glass-tube technique to confine the  $\text{P}_2\text{O}_5$  vapor. Dupree et al. (1989) clearly showed that quench rate exerts an important control on  $^{60}\text{Si}$  content for glasses of the same composition. Their results for  $\text{Na}_2\text{O}\cdot 2\text{SiO}_2\cdot 4\text{P}_2\text{O}_5$  suggest that  $^{60}\text{Si}$  is either not stable or present in greatly reduced amounts in the  $\text{P}_2\text{O}_5$ -rich silicate-phosphate melt and forms preferentially in the solid (glass and crystalline) products. Therefore, the bimodal distribution of structural states in the present  $\text{P}_2\text{O}_5$ -rich glasses (Fig. 7) could be due to a marked sensitivity to cooling rate during quenching. Even though our samples were quenched in water, they were not quenched in a reproducible manner, largely because quenching was inhibited by the sealed silica glass tube. The absence of intermediate structural states (Fig. 7) at constant composition is surprising and inconsistent with Dupree et al. (1989). The short experiment times required to preserve the integrity of the sealed silica glass tubes may have

resulted in incomplete reaction in the melts of  $^{69}\text{Si}$ -bearing glasses. However, this was not evident using the present methods of characterization: All materials investigated were single-phase, homogeneous glasses on the optical, EMPA, and XRD scales of resolution.

### Comparison of Si *K*- and *L*-edge XANES with $^{29}\text{Si}$ MAS NMR

The technique of  $^{29}\text{Si}$  MAS NMR spectroscopy has been established as a powerful means of studying coordination geometries and local structure of Si and the polymerization of  $\text{SiO}_4$  clusters in silicate glasses. As shown above, both Si *K*- and *L*-edge XANES spectra indicated that a proportion of the Si atoms are present in octahedral coordination in both  $\text{SiO}_2\text{-P}_2\text{O}_5$  and  $\text{Na}_2\text{O-SiO}_2\text{-P}_2\text{O}_5$  glasses containing more than 32 mol%  $\text{P}_2\text{O}_5$ , and qualitatively the content of  $^{69}\text{Si}$  increases proportionally with increase in the content of  $\text{P}_2\text{O}_5$ . These results are consistent with  $^{29}\text{Si}$  MAS NMR spectra for similar silicate-phosphate glasses (Dupree et al. 1987, 1989; Sekiya et al. 1988). Discrepancies with Dupree et al. (1989) for  $\text{SiO}_2\text{-P}_2\text{O}_5$  compositions are probably related to the difference in structural state of the glasses in the two studies rather than to the methods of structural characterization. Thus, Si *K*- and *L*-edge XANES spectra can provide information on coordination geometries and local structure of Si (Li et al. 1994a, 1994b, 1995a) and on the polymerization of  $\text{SiO}_4$  clusters (Li et al. 1995b) comparable to that from  $^{29}\text{Si}$  MAS NMR spectroscopy. In general,  $^{29}\text{Si}$  MAS NMR requires a larger sample size ( $\sim 1$  g), because of the low natural abundance of  $^{29}\text{Si}$ , but gives greater spectral resolution of  $^{69}\text{Si}$  and  $^{67}\text{Si}$  features. However, Si *K*- and *L*-edge X-ray absorption spectroscopy offers many advantages, particularly, small sample size ( $\sim 10$  mg), rapid acquisition of high-resolution XANES spectra, and complementary extended X-ray absorption fine-structure (EXAFS) data.

### ACKNOWLEDGMENTS

We thank two anonymous reviewers for helpful comments, and Y. Pan, Department of Geological Sciences, University of Saskatchewan, for EMPA. We also acknowledge X.H. Feng and K.H. Tan, Canadian Synchrotron Radiation Facility, and staff of the Synchrotron Radiation Center (SRC), University of Wisconsin, for their technical assistance, and the National Science Foundation (NSF) for support of the SRC. This work was supported by NSERC.

### REFERENCES CITED

- Bancroft, G.M. (1992) New development in far UV, soft X-ray research at the Canadian Synchrotron Radiation Facility. *Canadian Chemical News*, 44, 15–22.
- Chakraborty, I.N., and Condrate, R.A., Sr. (1985) The vibrational spectra of glasses in the  $\text{Na}_2\text{O-SiO}_2\text{-P}_2\text{O}_5$  system with a 1:1  $\text{SiO}:\text{P}_2\text{O}_5$  molar ratio. *Physics and Chemistry of Glasses*, 26, 68–73.
- Dickinson, J.E., Jr., and De Jong, B.H.W.S. (1988) Hydrogen-containing glass and gas-ceramic microfoam: Raman, XPS and MS-NMR results on the structure of precursor  $\text{SiO}_2\text{-B}_2\text{O}_3\text{-P}_2\text{O}_5$  glasses. *Journal of Non-Crystalline Solids*, 102, 196–204.
- Dingwell, D.B., Knoche, R., and Webb, S.L. (1993) The effect of  $\text{P}_2\text{O}_5$  on the viscosity of hepgoganitic liquid. *European Journal of Mineralogy*, 5, 133–140.
- Dupree, R., Holland, D., and Mortuza, M.G. (1987) Six-coordinated silicon in glasses. *Nature*, 328, 416–417.
- Dupree, R., Holland, D., Mortuza, M.G., Collins, J.A., and Lockyer, M.W.G. (1989) Magic angle spinning NMR of alkali phospho-alumino-silicate glasses. *Journal of Non-Crystalline Solids*, 127, 111–119.
- Finger, L.W., and Hazen, R.M. (1991) Crystal chemistry of six-coordinated silicon: A key to understanding the Earth's deep interior. *Acta Crystallographica*, B47, 561–580.
- Fröba, M., Wong, J., Behrens, P., Sieger, P., Rowen, M., Tanaka, T., Rek, Z., and Felsche, J. (1995a) Correlation of multiple scattering features in XANES spectra of Al and Si *K* edges to the Al-O-Si bond angle in aluminosilicate sodalites: An empirical study. *Physica B*, 208 and 209, 65–67.
- Fröba, M., Wong, J., Rowen, M., Brown, G.E., Jr., Tanaka, T., and Rek, Z. (1995b) Al and Si *K* absorption edges of  $\text{Al}_2\text{SiO}_5$  polymorphs using the new YB<sub>66</sub> soft X-ray monochromator. *Physica B*, 208 and 209, 555–556.
- Gan, H., and Hess, P.C. (1992) Phosphate speciation in potassium aluminosilicate glasses. *American Mineralogist*, 77, 495–506.
- Gan, H., Hess, P.C., and Kirkpatrick, R.J. (1994) Phosphorus and boron speciation in  $\text{K}_2\text{O-B}_2\text{O}_3\text{-SiO}_2\text{-P}_2\text{O}_5$  glasses. *Geochimica et Cosmochimica Acta*, 58, 4633–4647.
- Hess, P.C. (1991) The role of high field strength cations in silicates melts. In *Advances in Physical Geochemistry*, 9, 153–191.
- Ito, E., and Takahashi, T. (1987) Ultrahigh-pressure phase transformations and the constitution of the deep mantle. In *High-Pressure Research in Mineral Physics*, Geophysical Monograph, 39, 221–229.
- Jeanloz, R. (1990) The nature of the Earth's core. *Annual Review of the Earth and Planetary Sciences*, 18, 357–386.
- Klug, H., and Alexander, L.E. (1974) X-ray diffraction procedures: For polycrystalline and amorphous materials, 966 p. Wiley, New York.
- Kushiro, I. (1975) On the nature of silicate melt and its significance in magma genesis: Regularities in the shift of the liquidus boundaries involving olivine, pyroxene, and silica minerals. *American Journal of Science*, 275, 411–431.
- Lagarde, P., Flank, A.M., Tourillon, G., Liebermann, R.C., and Itie, J.P. (1992) X-ray absorption near edge structure of quartz: Application to the structure of densified silica. *Journal de Physiques I*, 2, 1043–1050.
- Li, Dien, Bancroft, G.M., Kasrai, M., Fleet, M.E., Feng, X.H., and Tan, K.H. (1994a) High-resolution Si and P *K*- and *L*-edge XANES spectra of crystalline  $\text{SiP}_2\text{O}_6$  and amorphous  $\text{SiO}_2\text{-P}_2\text{O}_5$ . *American Mineralogist*, 79, 785–788.
- Li, Dien, Bancroft, G.M., Kasrai, M., Fleet, M.E., Secco, R.A., Feng, X.H., Tan, K.H., and Yang, B.X. (1994b) X-ray absorption spectroscopy of silicon dioxide ( $\text{SiO}_2$ ) polymorphs: The structural characterization of opal. *American Mineralogist*, 79, 622–632.
- Li, Dien, Fleet, M.E., Bancroft, G.M., Kasrai, M., and Pan, Y. (1995a) Local structure of Si and P in  $\text{SiO}_2\text{-P}_2\text{O}_5$  and  $\text{Na}_2\text{O-SiO}_2\text{-P}_2\text{O}_5$  glasses: A XANES study. *Journal of Non-Crystalline Solids*, 188, 181–189.
- Li, Dien, Bancroft, G.M., Fleet, M.E., and Feng, X.H. (1995b) Silicon *K*-edge XANES spectra of silicate minerals. *Physics and Chemistry of Minerals*, 22, 115–122.
- Liebau, F. (1985) *Structural chemistry of silicates*, 347 p. Springer-Verlag, Berlin.
- Liu, L.G. (1975) Post-oxide phases of olivine and pyroxene and mineralogy of the mantle. *Nature*, 258, 510–512.
- London, D. (1987) Internal differentiation of rare element pegmatites: Effect of boron, phosphorus and fluorine. *Geochimica et Cosmochimica Acta*, 51, 403–420.
- (1992) Phosphorus in S-type magmas: The  $\text{P}_2\text{O}_5$  content of feldspars from peraluminous granites, pegmatites, and rhyolites. *American Mineralogist*, 77, 126–145.
- London, D., Cerný, P., Loomis, J.L., and Pan, J.J. (1990) Phosphorus in alkali feldspars of rare-element granitic pegmatites. *Canadian Mineralogist*, 28, 771–786.
- London, D., Morgan, G.B., IV, Babb, H.A., and Loomis, J.L. (1993) Behavior and effects of phosphorus in the system  $\text{Na}_2\text{O-K}_2\text{O-Al}_2\text{O}_3\text{-SiO}_2\text{-P}_2\text{O}_5\text{-H}_2\text{O}$  at 200 MPa ( $\text{H}_2\text{O}$ ). *Contributions to Mineralogy and Petrology*, 113, 450–465.
- Miya, T., Nakahara, M., and Inagaki, N. (1983) Single-mode fiber fabri-

- cation techniques for large capacity transmission systems. *Reviews in Electronic Communication Laboratory*, 31, 310–320.
- Mysen, B.O., Ryerson, F.J., and Virgo, D. (1981) The structural role of phosphorus in silicate melts. *American Mineralogist*, 66, 106–117.
- Nelson, C., and Tallant, D.R. (1984) Raman studies of sodium silicate glasses with low phosphate contents. *Physics and Chemistry of Glasses*, 25, 31–38.
- Okura, T., Inoue, H., and Kanazawa, T. (1990) Molecular orbital calculation of  $\text{SiK}\alpha$  chemical shift due to coordination in silicates and silico-phosphates. *Spectrochimica Acta*, 45B, 711–717.
- Ryerson, F.J., and Hess, P.C. (1978) Implications of liquid-liquid distribution coefficients to mineral-liquid partitioning. *Geochimica et Cosmochimica Acta*, 42, 921–932.
- (1980) The role of  $\text{P}_2\text{O}_5$  in silicate melts. *Geochimica et Cosmochimica Acta*, 44, 611–624.
- Sekiya, T., Mochida, N., Ohtsuka, A., and Uchida, K. (1988) 6-Coordinated  $\text{Si}^{4+}$  in  $\text{SiO}_2$ - $\text{PO}_{3/2}$  glasses— $^{29}\text{Si}$  MAS NMR method. *Nippon Seramik-kusu Kyokai Gakujutsu Ronbunshi*, 96, 571–573.
- Shibata, N., Horigudhi, M., and Edahiro, T. (1981) Raman spectra of binary high-silica glasses and fibers containing  $\text{GeO}_2$ ,  $\text{P}_2\text{O}_5$  and  $\text{B}_2\text{O}_3$ . *Journal of Non-Crystalline Solids*, 45, 115–126.
- Sutherland, D.G.J., Kasrai, M., Bancroft, G.M., Liu, Z.F., and Tan, K.H. (1993) Si *L*- and *K*-edge X-ray-absorption near-edge spectroscopy of gas-phase  $\text{Si}(\text{CH}_3)_x(\text{OCH}_3)_{4-x}$ : Models for solid-state analogs. *Physical Review B*, 48, 14989–15001.
- Swanson, D.K., and Prewitt, C.T. (1983) The crystal structure of  $\text{K}_2\text{Si}^{IV}\text{Si}_3^{\text{VI}}\text{O}_9$ . *American Mineralogist*, 68, 581–585.
- Tyliszczak, T. (1992) BAN data analysis program.
- Visser, W., and Koster van Groos, A.F. (1979) Effects of  $\text{P}_2\text{O}_5$  and  $\text{TiO}_2$  on liquid-liquid equilibria in the system  $\text{K}_2\text{O}$ - $\text{FeO}$ - $\text{Al}_2\text{O}_3$ - $\text{SiO}_2$ . *American Journal of Science*, 279, 970–988.
- Watson, E.B. (1976) Two liquid partition coefficients: Experimental data and geochemical implications. *Contributions to Mineralogy and Petrology*, 56, 119–134.
- Weeding, T.L., De Jong, B.H.W.S., Veeman, W.S., and Aitken, B.G. (1985) Silicon coordination changes from 4-fold to 6-fold on devitrification of silicon phosphate glass. *Nature*, 318, 352–353.
- Wong, J., and Angell, C.A. (1976) Glass structure by spectroscopy, 436 p. Marcel Dekker, New York.
- Wyllie, P.J., and Tuttle, O.G. (1964) Experimental investigation of silicate systems containing two volatile components: III. The effects of  $\text{SO}_2$ ,  $\text{P}_2\text{O}_5$ ,  $\text{HCl}$ , and  $\text{Li}_2\text{O}$  in addition to  $\text{H}_2\text{O}$ , on the melting temperatures of albite and granite. *American Journal of Science*, 262, 930–939.
- Yang, B.X., Middleton, F.H., Olsson, B.G., Bancroft, G.M., Chen, J.M., Sham, T.K., Tan, K.H., and Wallace, J.D. (1992) The design and performance of a soft X-ray double crystal monochromator beamline at Aladdin. *Nuclear Instruments and Methods in Physics Research*, A316, 422–436.
- Zachariasen, W.H. (1932) The atomic arrangement in glass. *Journal of American Chemical Society*, 54, 3841–3851.

MANUSCRIPT RECEIVED MARCH 31, 1995

MANUSCRIPT ACCEPTED SEPTEMBER 12, 1995